

Theoretical characterization of structural disorder in the tetramer model structure of eumelanin

Oleg Sapunkov, Abhishek Khetan, Vikram Pande, and Venkatasubramanian Viswanathan^{*}

Department of Mechanical Engineering, Carnegie Mellon University, 5000 Forbes Avenue, Pittsburgh, Pennsylvania 15213, USA



(Received 25 February 2019; revised manuscript received 17 June 2019; published 7 October 2019)

Eumelanin is regarded to be an attractive candidate material for biomedical applications. Despite many theoretical studies exploring the structure of eumelanin, an exact mapping of the energetic landscape of the very large phase space of eumelanin is still elusive. In this work, we implement a piecewise Ising model to predict formation enthalpies of eumelanin single and double tetramers, and demonstrate its superior predictive and generalizable capabilities. We believe this model will prove very useful in theoretically characterizing the many unique properties attributed to its disorder. The modular nature of the predictive Ising model built up in this work is well-suited for analysis and characterization of a larger phase space of eumelanin polymers, including hexamers and octomers, as well as larger stacked structures, such as potential triple and quadruple eumelanin tetramers. Absorbance data can be incorporated with populationwide predictions of polymer abundance to produce weighted-average predictions of broadband absorbance of bulk eumelanin.

DOI: [10.1103/PhysRevMaterials.3.105403](https://doi.org/10.1103/PhysRevMaterials.3.105403)

I. INTRODUCTION

Eumelanin is a subgroup of melanin pigments found in living organisms that plays an important role in skin coloration and UV protection [1]. The precise chemical structure of eumelanin is still not completely known because it is highly cross-linked and insoluble in available solvents [2]. Among organic polymers, eumelanin occupies a unique position because of (i) its widespread occurrence in nature, from people and mammals to fish, birds, and mollusks [3]; (ii) the variety of biological roles, from photoprotection to scavenging of reactive oxygen species [4,5] and metal chelation [6]; and (iii) distinct physical and chemical properties, including broadband photoabsorption throughout the visible range [7], water-dependent ionic-electronic semiconductorlike behavior [8], stable free-radical character, and efficient nonradiative energy dissipation [9], making eumelanin an attractive candidate for biomedical and technological applications. Despite growing interest in eumelanin-type functional materials and systems, the exact structural underpinnings due to the highly insoluble and heterogeneous character of these polymers has proved challenging [10].

In parallel, interest in miniaturized medical implants and edible biometric sensors has led to a need to develop novel biodegradable batteries, based on eumelanin extracted from the common cuttlefish (*Sepia officinalis*) [11,12]. Electrochemical characterization indicates the possibility of electrochemical intercalation of up to two sodium ions per eumelanin unit [11]. The theoretical analysis in the work of Kim *et al.* [11] utilizes a stacked tetramer model to rationalize these findings, originally proposed by Kaxiras *et al.* [13]. Recently, another study has explored the geometric complexity possible within the Kaxiras-Meng model [14–16]. While these studies represent important strides, a complete energetic landscape of double tetramer is still elusive given the large phase space.

Systematic exploration of large phase spaces for crystalline materials is enabled through the Ising model (or cluster expansion) [17–19]. The general methodology involves calculating the system energy for a subset of structures and training a model that can be used to then subsequently predict the rest of the phase space with very high accuracy. In this work, we develop an Ising model to describe the interactions in plane and out of plane for a double tetramer. Utilizing 108 density-functional-theory calculations, we train an Ising model that predicts on a test set with an accuracy of 0.15 eV. The model is generalizable and allows for an accurate mapping of the energetic landscape of a double tetramer. We believe this analysis can form the basis for further characterization of broadband absorbance, electrochemical ion intercalation, etc.

II. METHODS

A. DFT simulations

In this work, the primary molecular structure considered for this study is a double eumelanin tetramer, building on the work of Kaxiras *et al.* [13]. While other possible structures such as hexamer [20,21] and octomer [22] are important, we have chosen to utilize the double tetramer structural model to demonstrate our methodology. As will be discussed later, this model can be extended to other possible structures of eumelanin, including more complex multipolymers.

The specific structures simulated for this study include three types of eumelanin monomers: hydroquinone (HQ), indolequinone (IQ), and quinone-methide (MQ) [23]. The fourth and final monomer type described by Kaxiras *et al.* quinone-imine (NQ), was not used in this study, since it is an isomer of MQ, and is reported to be of lower stability than MQ in recent literature, and is thus anticipated to be of lower concentration in bulk eumelanin [24]. In the context of planar tetramer assembly and ion intercalation, its structural difference is negligible, and thus it is expected to produce structures with similar formation enthalpies. While

^{*}venkvis@cmu.edu

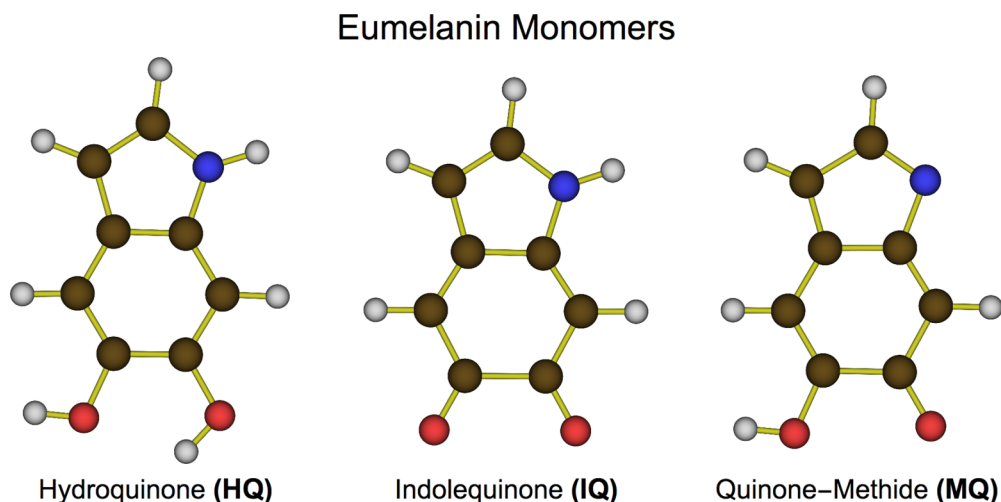


FIG. 1. Structures of the three primary eumelanin monomers used to form single and double tetramers investigated in the present study.

5,6-dihydroxyindole 2-carboxylic acid (DHICA) also forms a part of eumelanin oligomer, we have chosen to focus our analysis on HQ and its redox forms (MQ and IQ), similar to the work of Meng and Kaxiras [23]. The developed model can be easily extended to incorporate DHICA. The monomer structures are represented in Fig. 1.

We introduce the following naming scheme to describe the geometric arrangement of simulated structures. The double eumelanin tetramers are planar in the X - Y plane, stacked one above the other along the Z axis. This is one of the stable stacked structures when van der Waals (vdW) interactions are taken into account [11]. Looking down the Z axis onto the X - Y plane, the monomers of the lower tetramer are named first, starting with the monomer in quadrant 2 and proceeding clockwise. Following the four monomers of the lower tetramer, the four monomers of the upper tetramer are named in the same order. All monomers are designated by the first letter of their acronym (H for hydroquinone, I for

indolequinone, M for quinone-methide). Thus, for instance, in an example tetramer HHHM-HHHM, the two sets of three hydroquinones, in quadrants 2, 1, and 4, are situated one above the other, and the two sets of single quinone-methides, in quadrant 3, are likewise situated one above the other. Figure 2 illustrates the structures of an example planar tetramer and an example double tetramer.

In addition to simulations of the double eumelanin tetramer, single eumelanin planar tetramers were also simulated to compute formation enthalpies of the double tetramers from single tetramers. As will be discussed later, the purpose of these calculations was to ensure the out-of-plane interactions between the simulated pairs of planar double tetramers were properly quantified and accounted for. Finally, single eumelanin monomers were also simulated to compute formation enthalpies of both the single and double eumelanin tetramers. These single monomers were simulated in their stable stand-alone configuration with an additional two hydrogen atoms,

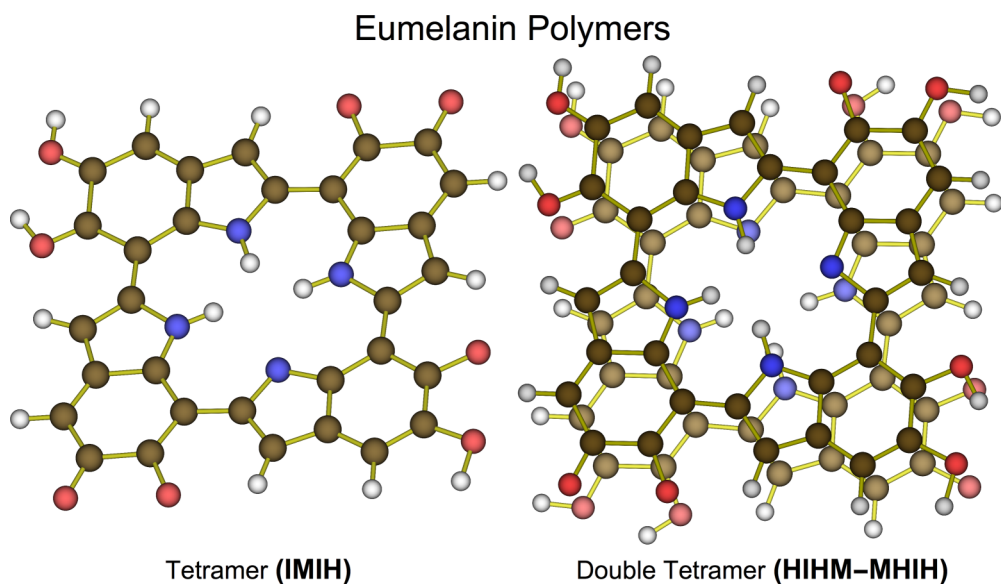


FIG. 2. Examples of a eumelanin tetramer and eumelanin double tetramer, showing the planar arrangement of monomers within tetramers and the parallel sheet stacking of tetramers.

which are lost in the polymerization process into tetramers, retained on the monomers.

Self-consistent density functional theory (DFT) calculations were performed using the projector augmented wave method as implemented in GPAW [25] with the Bayesian error estimation functional [26] with van-der-Waals correlation [27] (BEEF-vdW) exchange-correlation functional. All molecules were simulated in stand-alone bulk cells measuring $20 \times 20 \times 17 \text{ \AA}$, with all periodic boundary conditions disabled. Calculations were run with a real-space grid of 0.18 \AA . The conjugate gradient eigensolver was used to facilitate convergence of the simulations. Fermi-Dirac occupation smearing of 0.01 eV was used to expedite simulation convergence while providing accurate results. All structures were geometrically relaxed until the net force in the simulated molecule was decreased to 0.05 eV/\AA . The simulations were carried out at $1 \times 1 \times 1$ k -point sampling, following the Monkhorst-Pack scheme, as is the standard procedure for nonperiodic structures [28].

B. Formation enthalpies from bulk simulations

Several sets of formation enthalpies were calculated for the assemblage of simulated structures, including relevant monomers, planar tetramers, and double tetramers.

First, formation enthalpies of only the double tetramers (T-T) were calculated, using DFT-calculated internal energies of the double tetramers and DFT-calculated reference energies for the constituent elemental species: carbon, hydrogen, nitrogen, and oxygen:

$$\Delta H_{T-T}^a = U_{T-T}^{\text{DFT}} - \sum_C E_C^{\text{Ref}} - \sum_H E_H^{\text{Ref}} - \sum_N E_N^{\text{Ref}} - \sum_O E_O^{\text{Ref}} + \Delta pV. \quad (1)$$

The pressure-volume work term, ΔpV , can be disregarded, as it is typically about five orders of magnitude smaller than internal energy contributions in formation enthalpy calculations [29,30].

Elemental reference energy for hydrogen was calculated using simply the DFT-calculated internal energy of hydrogen gas, H_2 . Elemental reference energy for carbon was calculated using bulk graphite [31]. The reference energies for oxygen and nitrogen, however, required additional correction, since both are well-known to be poorly described within DFT [32,33]. Oxygen reference energy was calculated using the standard water-reference scheme [34], using DFT-computed internal energies of water and hydrogen gas, as well as the experimental formation enthalpy of water:

$$E_O^{\text{Ref}} = U_{\text{H}_2\text{O}}^{\text{DFT}} - U_{\text{H}_2}^{\text{DFT}} - \Delta H_{\text{H}_2\text{O}}^{\text{Exp}}. \quad (2)$$

Nitrogen reference energy was calculated using a similar, ammonia-reference scheme [35], using DFT-computed internal energies of ammonia and hydrogen gas, as well as the experimental formation enthalpy of ammonia:

$$E_N^{\text{Ref}} = U_{\text{NH}_3}^{\text{DFT}} - \frac{3}{2}U_{\text{H}_2}^{\text{DFT}} - \Delta H_{\text{NH}_3}^{\text{Exp}}. \quad (3)$$

In addition to calculating formation enthalpies of the double tetramers from the elemental basis, formation enthalpies

of the single planar tetramers (T) and the single monomers (M) were also computed, using the same elemental basis:

$$\Delta H_T^a = U_T^{\text{DFT}} - \sum_C E_C^{\text{Ref}} - \sum_H E_H^{\text{Ref}} - \sum_N E_N^{\text{Ref}} - \sum_O E_O^{\text{Ref}}, \quad (4)$$

$$\Delta H_M^a = U_M^{\text{DFT}} - \sum_C E_C^{\text{Ref}} - \sum_H E_H^{\text{Ref}} - \sum_N E_N^{\text{Ref}} - \sum_O E_O^{\text{Ref}}. \quad (5)$$

C. Ising model coefficients

To map out the energetic interactions between the eumelanin monomers, both within the planar tetramers and across the planes of the double tetramers, we utilize a modified Ising Model for the lattice Hamiltonian. As implemented, the model consists of a lattice of N sites i , whose filling is described by occupation terms, σ_i . All terms within the Ising Model are calculated using formation enthalpies of the monomers and polymers, referenced to their constituent atomic species, as described above. The occupation energies, h , in this implementation of the Ising model, represent the formation enthalpies of the monomers directly. As there are three types of monomers used in the explored configuration space of eumelanin double tetramers, three types of occupation terms were used: h_H , h_I , and h_M , each term corresponding to the formation enthalpy of its corresponding monomer. In addition to the occupation terms h , energy contributions to the full polymer due to monomer-monomer interactions were captured by the interaction terms j . Several types of interaction terms are identified, separated into in-plane interactions between monomers situated in the same planar tetramer, j_i , and out-of-plane interactions between monomers situated in opposing tetramers, j_o . Within each category, interactions between monomers occupying nearby quadrants are accounted for, j_{in} and j_{on} , as well as interactions between monomers occupying diametrically opposed quadrants, j_{id} and j_{od} . Finally, interactions between monomers situated in opposing dimers but in the same geometric quadrant, one underneath another, are accounted for as j_{ou} . Thus, a total of five major types of interaction terms are used in the Ising Model: j_{in} , j_{id} , j_{ou} , j_{on} , j_{od} . Within each type of interaction term, there is further distinction as to the types of monomers involved, with the full set of permutations between H, I, and M accounted for: HH, HI, HM, II, IM, and MM.

Two schemes were used to calculate the above occupation and coupling terms for the Ising model. In the first scheme, the formation enthalpy data of eumelanin double tetramers, calculated through DFT simulations, was used to derive the full set of corresponding Ising model coefficients in a single step, through a least-squares regression fit using Wolfram Mathematica. Each double tetramer formation enthalpy was described as

$$\begin{aligned} \Delta H_{T-T}^a = & \sum_{(i)} h_i \sigma_i + \sum_{(ik)} j_{in,i,k} \sigma_i \sigma_k + \sum_{(ik)} j_{id,i,k} \sigma_i \sigma_k \\ & + \sum_{(ik)} j_{ou,i,k} \sigma_i \sigma_k + \sum_{(ik)} j_{on,i,k} \sigma_i \sigma_k + \sum_{(ik)} j_{od,i,k} \sigma_i \sigma_k. \end{aligned} \quad (6)$$

The second scheme broke down the calculation of Ising model coefficients into three distinct steps, using the formation enthalpies of the monomers, single tetramers, and double tetramers for each step, respectively. First, the formation enthalpies of the monomers were used to calculate the occupation terms h directly. A correction had to be implemented for hydrogen, since each monomer lost two hydrogen atoms when it was polymerized into a tetramer:

$$\Delta H_{M_i}^a - 2E_H^{\text{Ref}} = h_i \sigma_i. \quad (7)$$

Next, the formation enthalpies of the single planar tetramers were used to calculate the in-plane coupling coefficients j_i . The formation enthalpy of a single tetramer contains contributions both from the presence of individual monomers and their in-plane interactions:

$$\Delta H_T^a = \sum_{\langle i \rangle} h_i \sigma_i + \sum_{\langle ik \rangle} j_{in_i,k} \sigma_i \sigma_k + \sum_{\langle ik \rangle} j_{id_i,k} \sigma_i \sigma_k. \quad (8)$$

To isolate the energetic contributions of in-plane interactions, we subtracted the occupation-energy contributions of the constituent monomers, which were quantified in the preceding step, from the formation enthalpy of the tetramer. In effect, the formation enthalpy of a tetramer from the monomer basis was calculated. The resultant energy was used to calculate the in-plane coupling coefficients through a least-squares regression fit using Wolfram Mathematica:

$$\Delta H_T^a - \sum_{\langle i \rangle} h_i \sigma_i = \Delta H_T^M, \quad (9)$$

$$\Delta H_T^M = \sum_{\langle ik \rangle} j_{in_i,k} \sigma_i \sigma_k + \sum_{\langle ik \rangle} j_{id_i,k} \sigma_i \sigma_k. \quad (10)$$

Finally, the formation enthalpies of the double tetramers were used to calculate the out-of-plane coupling coefficients j_o . As discussed in the one-step scheme, the formation enthalpy of the double tetramer contains information about all types of occupation and coupling terms, so we subtracted the occupation-energy contributions, calculated using the monomers, and the in-plane interaction-energy contributions, calculated using the single tetramers. Effectively, the remaining energy represented the formation enthalpy of a double tetramer from its constituent single tetramers. This formation enthalpy was used to fit the out-of-plane interaction coefficients through a least-squares regression fit using Wolfram Mathematica:

$$\begin{aligned} \Delta H_{T-T}^a - \left(\sum_{\langle i \rangle} h_i \sigma_i + \sum_{\langle ik \rangle} j_{in_i,k} \sigma_i \sigma_k + \sum_{\langle ik \rangle} j_{id_i,k} \sigma_i \sigma_k \right) \\ = \Delta H_{T-T}^T, \end{aligned} \quad (11)$$

$$\Delta H_{T-T}^T = \sum_{\langle ik \rangle} j_{ou_i,k} \sigma_i \sigma_k + \sum_{\langle ik \rangle} j_{om_i,k} \sigma_i \sigma_k + \sum_{\langle ik \rangle} j_{od_i,k} \sigma_i \sigma_k. \quad (12)$$

D. Double tetramer phase space

Following the derivation of the interaction coefficients, these coefficients were applied to predict the formation enthalpies of the entire phase space of relevant eumelanin double

tetramers. If every possible permutation of HQ, IQ, and MQ within a double tetramer is considered, there exist a total of 6561 distinctly named double tetramers. However, many of these tetramers are simply rotated or flipped equivalents of other tetramers within the same phase space. To account for this phase space degeneracy, the full set of Ising model coupling coefficients for each of the 6561 configurations was calculated analytically, and families of configurations which matched the set of coupling coefficients had all but one member removed from the phase space. This left a total of 1032 distinct, nondegenerate double tetramer configurations in the phase space.

To provide training data for the Ising Model, a total of 85 double tetramers composed of HQ, IQ, and MQ monomers were simulated in DFT using the BEEF-vdW exchange-correlation functional. In addition, the three monomers themselves were simulated in DFT, as well as 20 intermediate single planar tetramers.

This study yielded two sets of interaction coefficients, as described above: one derived from the formation enthalpies of the double tetramers calculated directly from the atomic basis in one step, the other derived from the formation enthalpies of the double tetramers, single tetramers, and monomers, all calculated from the atomic basis, in three steps. The use of the BEEF-vdW exchange correlation functional generates a non-self-consistent ensemble of energies, which was used to train an ensemble of Ising models. It has been shown that the ensemble of energies reliably reproduces trends in energies at the generalized gradient approximation (GGA) level [36–39].

To most adequately represent the distribution of predicted formation enthalpies of the melanin double tetramers, it was decided to use a histogram plot of the calculated formation enthalpies predicted for every double tetramer configuration. To produce these plots, the double tetramers were sorted in order of increasing average formation enthalpy, as calculated across the full ensemble of 2000 values predicted by the BEEF-vdW functional. For every double tetramer, the standard deviation of formation enthalpy was calculated across all 2000 predicted BEEF-vdW values, to quantify uncertainty in the calculation. This calculated standard deviation was represented as a pair of whiskers on the histogram of formation enthalpies, centered on each individual column of the histogram. The whiskers provided for each column represent the standard deviation of formation enthalpies relevant only to the double tetramer structures present in that column. Since the standard deviation slightly differed for individual double tetramers, the resultant bands are slightly but negligibly different for each column.

III. RESULTS AND DISCUSSION

Using the one-step calculation for formation enthalpy of the double tetramers, it was found that the average formation enthalpy across all simulated double tetramers, calculated from the atomic reference basis, was -14.7 eV, with a standard deviation of 3.1 eV. Double tetramers containing a higher proportion of HQ were found to be the most stable, down to -19.3 eV, while double tetramers containing higher proportions of MQ exhibited the least negative formation enthalpies, up to -5.22 eV. The standard deviation of calculated

TABLE I. Statistics on calculated Ising model coefficient values, in eV, summarized across each general type of coefficient. Values reported for occupation terms h constitute a summary for three monomer-specific occupation coefficients, while values reported for interaction terms j constitute a summary for six double-monomer-specific coefficients. Grand means and grand standard deviations are provided for coefficients calculated using the one-step and the three-step calculation schemes, for a global overview comparing the fit coefficient magnitudes resulting from the two methods.

Coeff	Grand μ (1S)	Grand σ (1S)	Grand μ (3S)	Grand σ (3S)
h	-0.28	0.08	6.49	1.11
jin	-0.26	0.23	-4.03	0.24
jid	-0.46	0.30	-7.40	0.22
jou	-0.46	0.37	-0.14	0.17
jon	-0.20	0.23	-0.05	0.11
jod	-0.44	0.04	-0.12	0.06

formation enthalpy for each individual double tetramer throughout the phase space of the BEEF-vdW ensemble was calculated as well. The average of these standard deviations for the set of simulated structures was 2.9 eV, with an overall standard deviation of just 0.1 eV.

The average formation enthalpy of an individual planar tetramer, calculated from the atomic basis, was -5.09 eV, with a standard deviation of 1.92 eV. Thus, it was expected the formation enthalpy of the double tetramer from single planar tetramers would be of comparable order-of-magnitude to the formation enthalpy of the said tetramers. As calculated, the average formation enthalpy of a double tetramer from its constituent single tetramers was -1.88 eV, with a standard deviation of 0.58 eV. From this observation, it was apparent that the out-of-plane coupling coefficients derived through the Ising model should be lower than the in-plane coupling coefficients.

Finally, formation enthalpies of the individual monomers were calculated from the atomic basis. The average magnitude was found to be -1.46 eV, with a standard deviation of 1.11 eV. Since each corresponding h term, derived from the formation enthalpies of the monomers, had to account for the loss of two hydrogen atoms, the average magnitude of the occupation energies used in the three-step Ising model was 6.49 eV.

In both least-squares fits of the coupling coefficients used with the Ising Model, as fit to the training data, the reported r^2 was very high, in excess of 0.99, for all ensemble-specific sets of coefficients. However, the values derived for the coupling coefficients differed strongly between the two methods. A total of 33 coefficients are reported: three occupation coefficients h and 30 interaction coefficients j , the latter separated into five categories. For every one of the 33 coefficients, 2000 values were calculated, one for every value reported by the BEEF-vdW exchange-correlation functional. Table II provides a detailed report of all 33 coefficients, with mean values μ and standard deviations σ , calculated across all 2000 values provided by BEEF-vdW. Table I then gives a brief summary, comparing average magnitudes across all coefficients of a particular type: one category for occupation coefficients h and five categories for interaction coefficients j .

TABLE II. Statistics on calculated coefficient values, in eV, in the emelanin Ising model. Mean and standard deviation data provided for individual coefficients across the 2000 values exported with the BEEF-vdW ensemble, for Ising models computed using the three-step calculation scheme.

Coeff.	μ (3S)	σ (3S)
hH	5.23	1.21
hI	6.92	1.25
hM	7.33	1.29
jinHH	-3.82	0.56
jinHI	-3.89	0.56
jinHM	-4.32	0.57
jinII	-3.88	0.56
jinIM	-4.37	0.57
jinMM	-3.92	0.56
jidHH	-7.16	1.03
jidHI	-7.23	1.03
jidHM	-7.55	1.04
jidII	-7.24	1.03
jidIM	-7.68	1.04
jidMM	-7.56	1.03
jouHH	-0.18	0.1
jouHI	-0.43	0.14
jouHM	-0.17	0.14
jouII	-0.07	0.07
jouIM	-0.01	0.11
jouMM	0.04	0.09
jonHH	-0.11	0.06
jonHI	-0.17	0.05
jonHM	-0.06	0.06
jonII	0.11	0.09
jonIM	-0.1	0.05
jonMM	0.04	0.07
jodHH	-0.09	0.07
jodHI	-0.15	0.07
jodHM	-0.06	0.07
jodII	-0.08	0.09
jodIM	-0.11	0.07
jodMM	-0.23	0.05

It is evident that although both methods are able to match the formation enthalpies of the double tetramers well, the one-step calculation method provides a less physically interpretable model. In addition, this set of coupling coefficients fails to predict the formation enthalpies of single tetramers well. The predicted coefficient values using the one-step calculation are not generalizable as no data regarding the monomers and single-tetramers data were used in the training. It is worth highlighting that this one-step analysis would constitute a black-box application of the Ising model for double tetramer model.

On the other hand, the results provided by the three-step calculation method are far more systematic, generalizable, and physically meaningful. In the full set of fit Ising model coefficients, it was found that the occupation coefficients and the in-plane coupling coefficients contribute the bulk of the formation enthalpy of a double tetramer, as was expected since out-of-plane interactions are dominantly vdW interactions and do not involve any chemical bonding. Of the in-plane

This finding is in good agreement with recent work by Chen and Buelher [24], who found through an extensive *ab initio* phase space study of eumelanin polymers composed of IQ and MQ monomers that a selection of polymers built with a mixture of IQ and MQ monomers exhibit higher enthalpy of formation than polymers built purely from IQ monomers, even though the IQ monomer exhibits higher stability than the MQ monomer. Out-of-plane coefficients calculated from the Ising model indicate that the strongest interactions involve HQ monomers, either in combination with fellow HQ monomers or other monomers. This is expected, since the HQ-rich double tetramers were found to be the most stable structures investigated, stabilized both by the presence of HQ monomers and their out-of-plane interactions.

These observations have significant implications for the anticipated intercalation potentials of ions into these double tetramers, as one of the preferred locations for intercalation of ions is the double tetramer's inner ring. The HHHH-HHHH-type double tetramer carries eight hydrogen atoms protruding into the inner ring, which may hinder ion intercalation, while the IQ-rich and MQ-rich double tetramers carry fewer hydrogen atoms protruding into the inner ring, and may possess strong binding centers for ion intercalation.

Recent experimental and *ab initio* simulation work indicates that the eumelanin tetramer and the eumelanin stacked double tetramer play an important role in metal ion binding and broadband absorption of bulk eumelanin [11,13]. Our results are consistent with earlier work by Kaxiras *et al.* [13], where they show that HQ-rich phases of eumelanin display are consistently more stable than the eumelanin polymers, ranging from dimers to tetramers, as compared to polymers poor in HQ. The modular nature of the predictive Ising model built up in this work is well-suited for analysis and characterization of a larger phase space of eumelanin polymers, including hexamers and octomers, as well as larger stacked structures, such as potential triple and quadruple eumelanin tetramers. Furthermore, as the model allows for phase-space-wide prediction of relative stability of specific polymers, it

can be incorporated in a predictive model used to study the broadband absorbance of bulk eumelanin, by utilizing a weighted average of bulk polymer composition and calculated absorbance data. The effect of localization of electronic states [41,42] can be explored within this framework, which will be done in a future study. This can be used to compare against the experimental evidence from electron paramagnetic resonance spectra [43].

IV. CONCLUSIONS

In this study, we have built a generalizable, physically meaningful Ising model to describe the energetic interactions of eumelanin. This model allows a precise mapping of the very large phase of eumelanin structures within the double tetramer model. We highlight the importance of carrying out a stepwise training of the model coefficients using first the monomer enthalpies, followed by the single tetramer enthalpies and finally the double tetramer. The developed model will prove to be extremely useful in rapidly exploring the absorbance, ion intercalation of eumelanin within the double tetramer model. We also believe the developed methodology can be extended to other possible structural models for eumelanin such as the hexamer, octamer, etc.

ACKNOWLEDGMENTS

The computational portion of this work was performed on the Arjuna computer cluster, which was funded through Carnegie Mellon College of Engineering and the departments of Mechanical Engineering, Electrical and Computer Engineering, and Chemical Engineering. The computational portion of this work was performed on Hercules computer cluster, which was funded through a Carnegie Mellon College of Engineering Equipment grant. O.B.S. acknowledges support from the DoD SMART Fellowship. The authors thank Professor Christopher Bettinger of Carnegie Mellon University for helpful discussions on eumelanin structure and function.

-
- [1] P. S. Friedmann and B. A. Gilchrist, *J. Cell. Physiol.* **133**, 88 (1987).
 - [2] S. Ito, K. Wakamatsu, K. Glass, and J. D. Simon, *Anal. Biochem.* **434**, 221 (2013).
 - [3] N. P. Edwards, P. L. Manning, and R. A. Wogelius, *Pigment Cell Melanoma Res.* **27**, 684 (2014).
 - [4] J. B. Nofsinger, Y. Liu, and J. D. Simon, *Free Radicals Biol. Med.* **32**, 720 (2002).
 - [5] J. Bustamante, L. Bredeston, G. Malanga, and J. Mordoh, *Pigment Cell Melanoma Res.* **6**, 348 (1993).
 - [6] K. M. Im, T.-W. Kim, and J.-R. Jeon, *ACS Biomater. Sci. Eng.* **3**, 628 (2017).
 - [7] M. L. Tran, B. J. Powell, and P. Meredith, *Biophys. J.* **90**, 743 (2006).
 - [8] P. Meredith and T. Sarna, *Pigment Cell Melanoma Res.* **19**, 572 (2006).
 - [9] K.-Y. Ju, Y. Lee, S. Lee, S. B. Park, and J.-K. Lee, *Biomacromolecules* **12**, 625 (2011).
 - [10] M. d'Ischia, A. Napolitano, A. Pezzella, P. Meredith, and T. Sarna, *Angew. Chem. Int. Ed.* **48**, 3914 (2009).
 - [11] Y. J. Kim, A. Khetan, W. Wu, S.-E. Chun, V. Viswanathan, J. F. Whitacre, and C. J. Bettinger, *Adv. Mater.* **28**, 3173 (2016).
 - [12] Y. J. Kim, W. Wu, S.-E. Chun, J. F. Whitacre, and C. J. Bettinger, *Proc. Natl. Acad. Sci. USA* **110**, 20912 (2013).
 - [13] E. Kaxiras, A. Tsolakidis, G. Zonios, and S. Meng, *Phys. Rev. Lett.* **97**, 218102 (2006).
 - [14] E. Di Mauro, R. Xu, G. Soliveri, and C. Santato, *MRS Comm.* **7**, 141 (2017).
 - [15] E. Vahidzadeh, A. P. Kalra, and K. Shankar, *Biosens. Bioelectron.* **122**, 127 (2018).
 - [16] O. Crescenzi, M. d'Ischia, and A. Napolitano, *Biomimetics* **2**, 21 (2017).
 - [17] G. Ceder, *Comput. Mater. Sci.* **1**, 144 (1993).
 - [18] D. De Fontaine, M. Asta, G. Ceder, R. McCormack, and G. Van Tendeloo, *Europhys. Lett.* **19**, 229 (1992).

- [19] P. D. Tepesch, G. D. Garbulsky, and G. Ceder, *Phys. Rev. Lett.* **74**, 2272 (1995).
- [20] M. Randhawa, T. Huff, J. C. Valencia, Z. Younossi, V. Chandhoke, V. J. Hearing, and A. Baranova, *FASEB J.* **23**, 835 (2009).
- [21] K. B. Stark, J. M. Gallas, G. W. Zajac, J. T. Golab, S. Gidanian, T. McIntire, and P. J. Farmer, *J. Phys. Chem. B* **109**, 1970 (2005).
- [22] A. Slominski, D. J. Tobin, S. Shibahara, and J. Wortsman, *Physiol. Rev.* **84**, 1155 (2004).
- [23] S. Meng and E. Kaxiras, *Biophys. J.* **94**, 2095 (2008).
- [24] C.-T. Chen and M. J. Buehler, *Phys. Chem. Chem. Phys.* **20**, 28135 (2018).
- [25] J. Enkovaara, C. Rostgaard, J. J. Mortensen, J. Chen, M. Duřak, L. Ferrighi, J. Gavnholt, C. Glinsvad, V. Haikola, H. Hansen *et al.*, *J. Phys.: Condens. Matter* **22**, 253202 (2010).
- [26] J. J. Mortensen, K. Kaasbjerg, S. L. Frederiksen, J. K. Nørskov, J. P. Sethna, and K. W. Jacobsen, *Phys. Rev. Lett.* **95**, 216401 (2005).
- [27] J. Wellendorff, K. T. Lundgaard, A. Møgelhøj, V. Petzold, D. D. Landis, J. K. Nørskov, T. Bligaard, and K. W. Jacobsen, *Phys. Rev. B* **85**, 235149 (2012).
- [28] H. J. Monkhorst and J. D. Pack, *Phys. Rev. B* **13**, 5188 (1976).
- [29] M. K. Aydinol, A. F. Kohan, G. Ceder, K. Cho, and J. Joannopoulos, *Phys. Rev. B* **56**, 1354 (1997).
- [30] M. Obrovac and V. Chevrier, *Chem. Rev.* **114**, 11444 (2014).
- [31] V. Pande and V. Viswanathan, *Phys. Rev. Materials* **2**, 125401 (2018).
- [32] T. Jacob, *Fuel Cells* **6**, 159 (2006).
- [33] T. H. Rod, B. Hammer, and J. K. Nørskov, *Phys. Rev. Lett.* **82**, 4054 (1999).
- [34] J. D. Baran, H. Grönbeck, and A. Hellman, *J. Am. Chem. Soc.* **136**, 1320 (2014).
- [35] B. Wang and S. T. Pantelides, *Phys. Rev. B* **83**, 245403 (2011).
- [36] G. Houchins and V. Viswanathan, *Phys. Rev. B* **96**, 134426 (2017).
- [37] O. Vinogradova, D. Krishnamurthy, V. Pande, and V. Viswanathan, *Langmuir* **34**, 12259 (2018).
- [38] D. Krishnamurthy, H. A. Hansen, and V. Viswanathan, *ACS Ener. Lett.* **1**, 162 (2016).
- [39] D. Krishnamurthy, V. Sumaria, and V. Viswanathan, *J. Phys. Chem. Lett.* **9**, 588 (2018).
- [40] See Supplemental Material at <http://link.aps.org/supplemental/10.1103/PhysRevMaterials.3.105403> for details related to the formation enthalpy calculations through the one-step method.
- [41] D. S. Galvao and M. J. Caldas, *J. Chem. Phys.* **88**, 4088 (1988).
- [42] D. S. Galvao and M. J. Caldas, *J. Chem. Phys.* **93**, 2848 (1990).
- [43] J. V. Paulin, A. Batagin-Neto, and C. F. Graeff, *J. Phys. Chem. B* **123**, 1248 (2019).